

Supplemental Information

Biodegradable hydrogels with photodynamic antibacterial activity promote wound healing and mitigate scar formation

Chen Zhang^a, Dan Yang^a, Tai-Bao Wang^a, Xuan Nie^b, Guang Chen^b, Long-Hai Wang^b, Ye-Zi You^{b*}, Qin Wang^{a*}

^a Department of Otorhinolaryngology, Head and Neck Surgery, The First Affiliated Hospital of Anhui Medical University, Hefei, China.

^b Department of Polymer Science and Engineering, University of Science and Technology of China, Hefei, China.

*To whom correspondence should be addressed.

E-mail: wangqin@ahmu.edu.cn

E-mail: yzyou@ustc.edu.cn

Supplementary Results

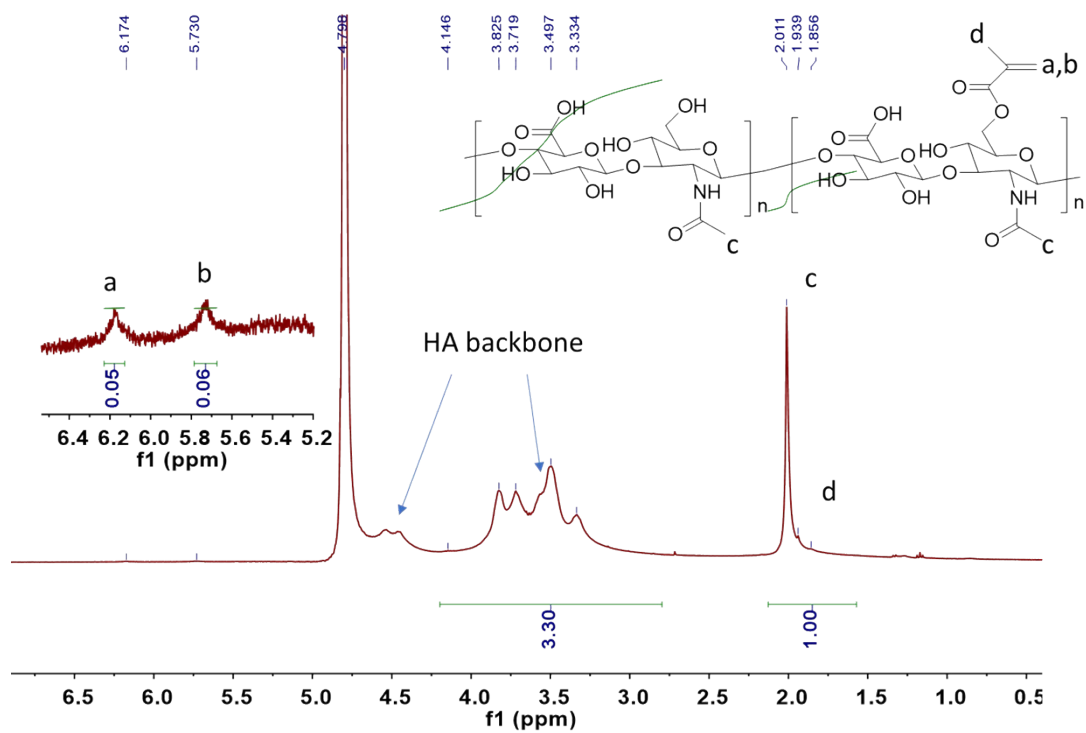


Figure S1. ^1H NMR spectrum of HA-ene.

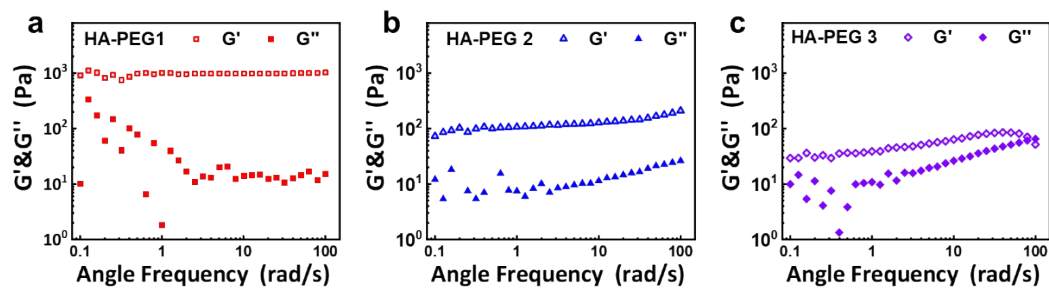


Figure S2. Rheology data (value of G' and G'' of the hydrogel according to frequency) of HA hydrogel with different crosslinking degrees (The hyaluronic acid hydrogels prepared using 0.1, 0.2, and 0.3 g 10 wt% 4-arm PEG-SH solution were denoted as HA-PEG1, HA-PEG2 and HA-PEG3, respectively).

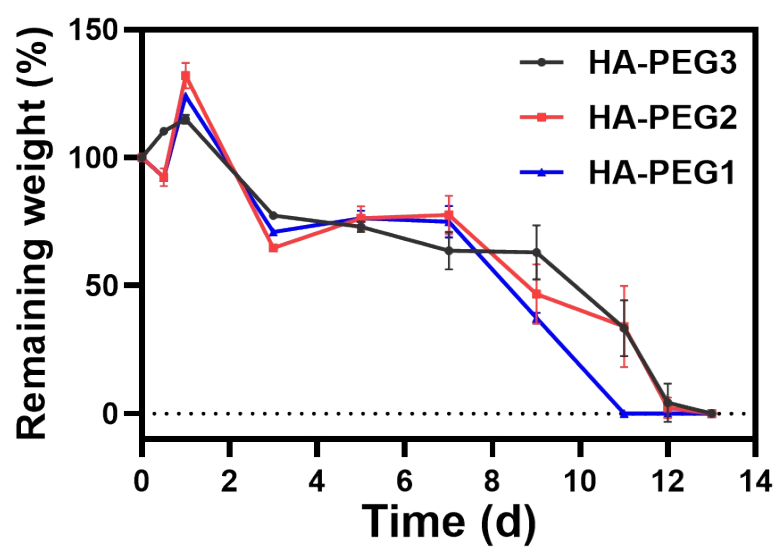


Fig. S3. The degradation of hydrogels in the presence of hyaluronidase solution.

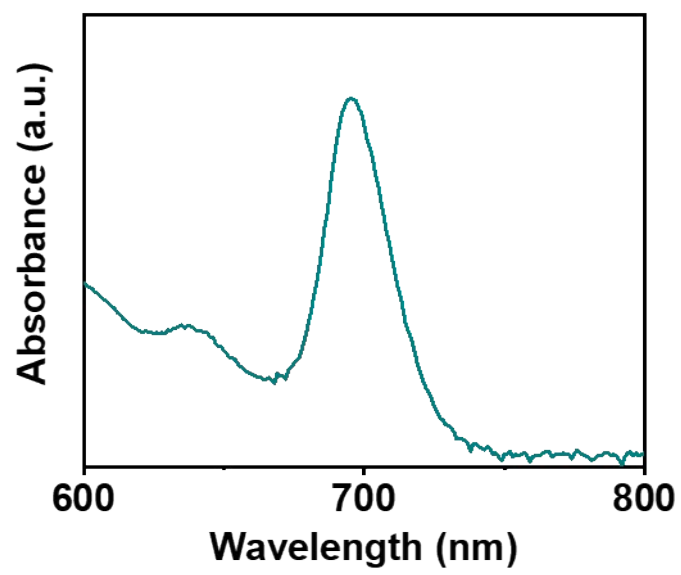


Figure S4. UV-vis absorption of VP.

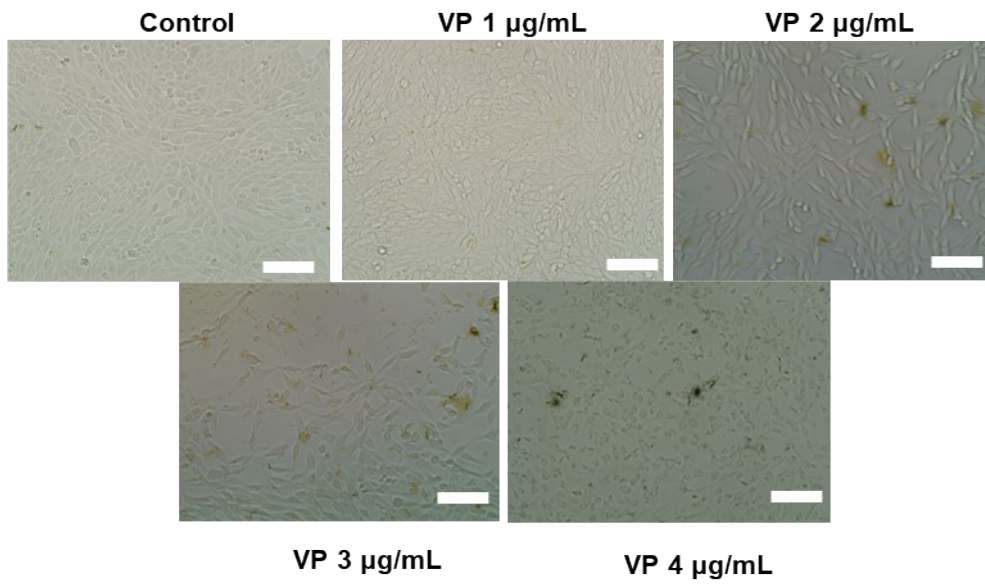


Figure S5. Cell morphology of 3T3 cells cultured with different concentrations of verteporfin (Scale bar: 200 µm).

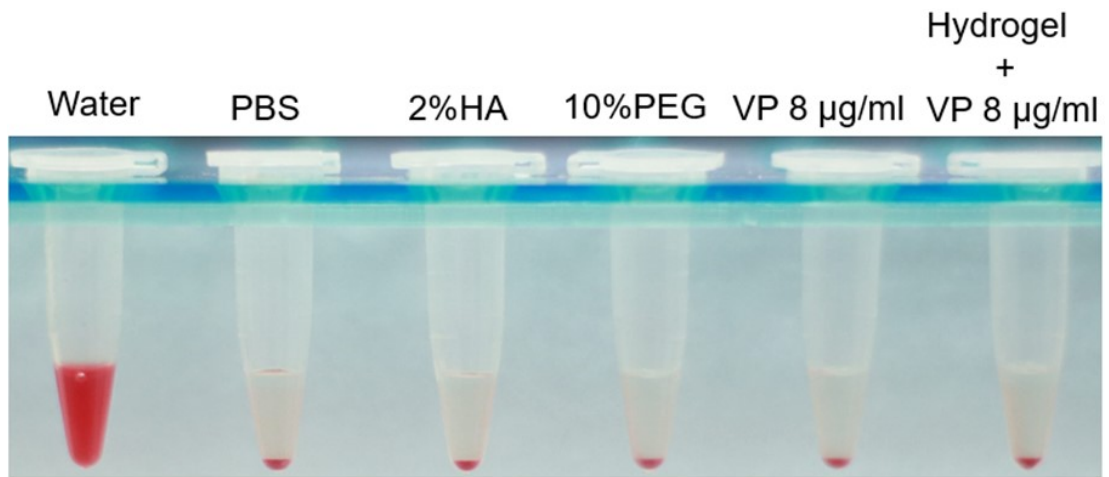


Figure S6. Hemolytic properties of all the components of VP-gel.

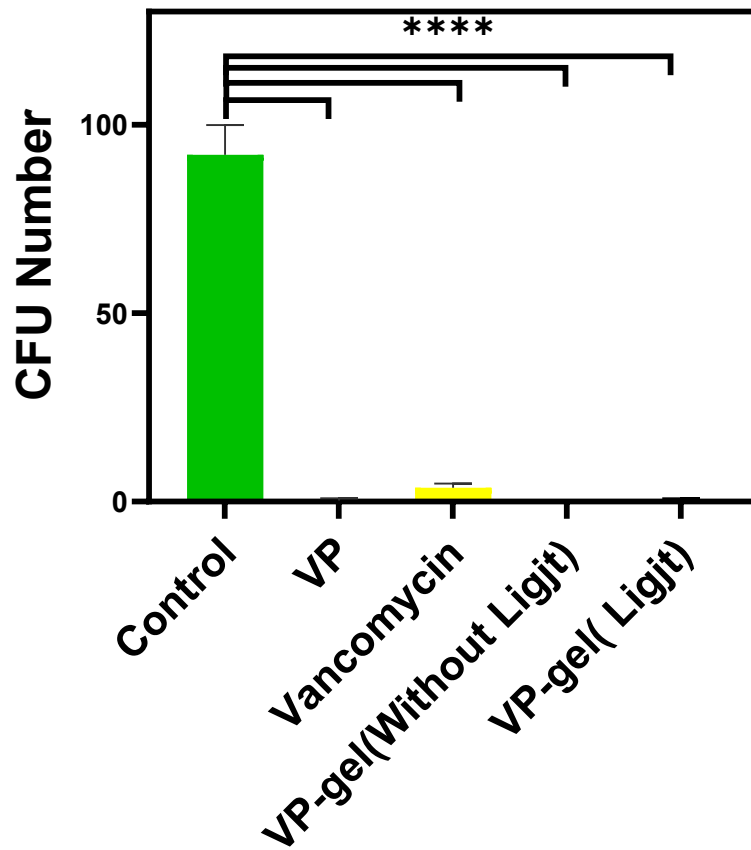


Figure S7. The histogram of the colony forming unit (CFU) number for MRSA was measured after growth on agar plates for a period of 24 h at 37 °C. All data are presented as the mean \pm SD (n = 3, *p < 0.05). All statistical analyses were performed by Student's t test.

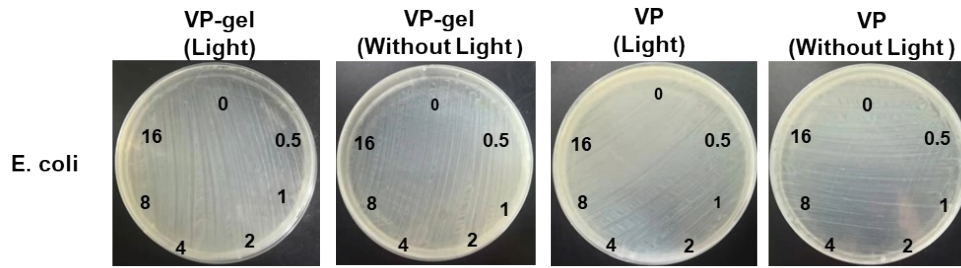


Fig. S8. Antibacterial activity of VP solution and VP-gel against *E. coli*. The labeled numbers in plates indicate the VP concentration ($\mu\text{g/mL}$).

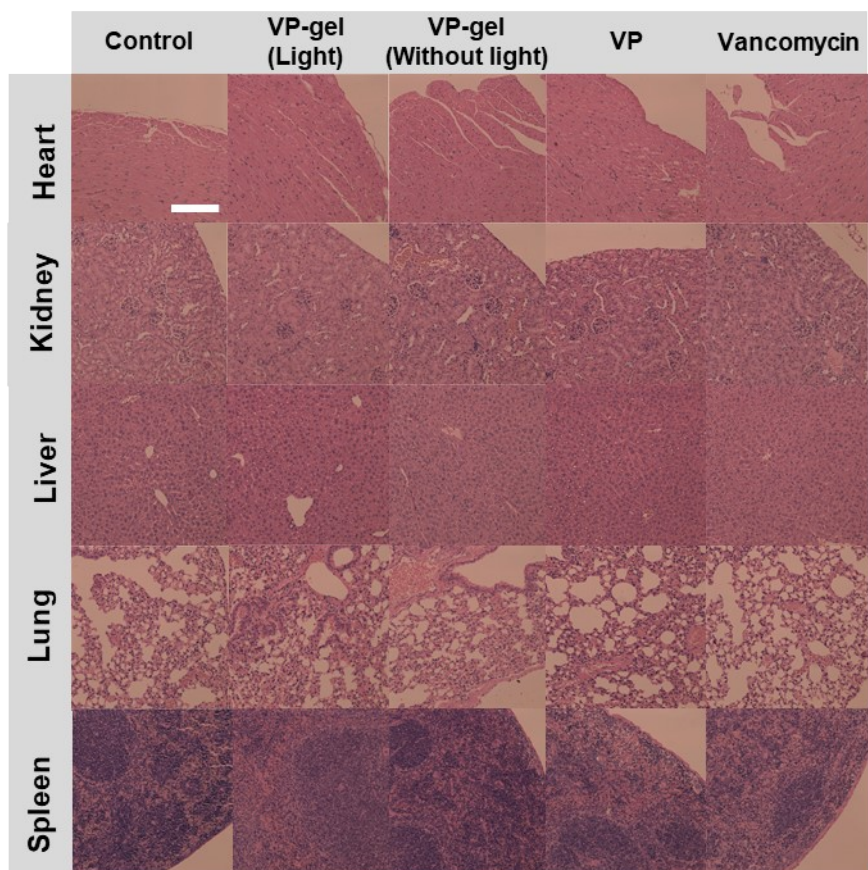


Figure S9. H&E staining images of tissue slices of major organs (heart, liver, spleen, lung, and kidney) with different treatment. Scale bar: 200 μ m.